

https://doi.org/10.1070/QEL16318

Dispersion management of the SULF front end

Shuai Li, Cheng Wang, Yanqi Liu, Yi Xu, Zhengzheng Liu, Jun Lu, Yanyan Li, Xingyan Liu, Zhaoyang Li, Yuxin Leng, Ruxin Li

Abstract. **To manage dispersion of the front end in the Shanghai Superintense Ultrafast Laser Facility (SULF), which is a large-scale project aimed at delivering 10 PW laser pulses, a stretcher based on a combination of a grating and a prism (grism) pair is inserted between an Öffner-triplet-type stretcher and a regenerative amplifier to reduce high-order dispersion introduced by optical materials at the amplification stage. The alignment of the grism pair is implemented by controlling the far-field pattern of the output beam of the grism pair. The energy of the front end reaches up to 7 J at a 1-Hz repetition rate. Experimental results show that the pulse duration can be compressed to 22.4 fs and the spectral distortion over the spectrum is less than 2.25 rad.**

Keywords: *pulse compression, dispersion compensation devices, grism.*

1. Introduction

The chirped-pulse amplification (CPA) technique and its analogue, optical parametric chirped-pulse amplification (OPCPA), have been used to generate laser pulses with a high intensity and ultrashort pulse duration [1–3]. Such ultrahigh-peak-power laser systems greatly benefit fundamental research areas that involve acceleration of charged particles (electrons and protons) and generation of high-energy photon (X-ray and γ-ray) sources [4]. The basic principle of the techniques is to stretch a seed pulse in the time domain and to compress it to its initial duration after amplification. This could improve the extraction efficiency and reduce the damage risk caused by nonlinear effects during the amplification stage. In 1999, the first CPA petawatt laser system based on Nd:glass was built at the Lawrence Livermore National Laboratory (LLNL, USA) [5]. Later in 2003, the first 0.85 PW, 33 fs laser pulse was produced by the Japan Advanced Photon Research Center (APRC) [6]. Since then, a global race to build petawatt or even higher-power laser systems with a pulse duration of few tens of femtosecond has been initiated. In femtosecond petawatt laser systems recently completed or currently under construction [7–9], high-order dispersion compensation is still the bottleneck to achieve a near Fourier-transform-limited (FTL) pulse, which could further improve the peak intensity of the laser systems. Dispersion management is of great significance for such ultrahigh-power systems [10].

In general, the effect of higher-order dispersion can be partially balanced by introducing proper negative third-order dispersion (TOD), so that a shorter output pulse can be achieved [11]. Based on this theory, the duration of the compressed pulse in our 2.0-PW Ti:sapphire laser system developed at the Shanghai Institute of Optics and Fine Mechanics (SIOM) in 2013 was 26 fs [9]. However, the compressed pulse was not as near the FTL pulse as possible. The group delay dispersion (GVD) could be reduced to zero easily, while the third-order and fourth-order dispersion (FOD) was not compensated for completely. Such elements as a acousto-optic programmable dispersive filter (AOPDF) [12] and a deformable mirror [13] are widely used for pulse compression in laser systems. The AOPDF has a large group-delay range that extends over 3 ps, and arbitrary phase and amplitude profiles can be applied to an ultrashort pulse by using this element. However, the residual phase of a petawatt CPA system is generally beyond the compensation range of an AOPDF, and this element has a low damage threshold. An advantage of a deformable mirror is a possibility of smoothly varying phase modulation, with low losses (97% reflection) and relatively high actuator density, but its dynamic range is very limited.

Efficient reflection grisms for pulse-compression and material-dispersion compensation have been demonstrated for 800-nm laser pulses. The grism is a combination of a grating and a prism. For a grism pair, GVD and FOD are negative, while the sign of TOD depends on the design [14]. An additional degree of freedom in the grism compressor relies on the tilt of the prisms with respect to the planes of the gratings [15]. Such compressors can be matched to compensate for the dispersion of bulk/fiber stretchers (and/or laser amplifiers) up to the fourth order, and the residual phase is mainly limited to the fifth order. Despite this, the dispersion system with a small stretching ratio is not suitable for ultrahigh power laser systems, because the stretching ratio is generally more than 10000 in high power laser systems.

In 2015, we demonstrated a stable and economical passive dispersion compensation method to completely rule out

Shuai Li. Chinese Academy of Sciences, Shanghai Institute of Optics and Fine Mechanics, State Key Laboratory of High Field Laser Physics, Shanghai 201800, China; University of Chinese Academy of Sciences, Beijing 100049, China;
Cheng Wang, Yanqi Liu, Yi Xu, Zhengzheng Liu, Jun Lu, Yanyan Li, Xingyan Liu. Chinese Academy of Sciences, Shanghai Institute of Optics and Fine Mechanics, State Key Laboratory of High Field Laser Physics, Shanghai 201800, China;
Zhaoyang Li. Osaka University, Institute of Laser Engineering, 2-6 Yamadaoka, Suita, Osaka 565-0871, Japan;
Yuxin Leng, Ruxin Li. Chinese Academy of Sciences, Shanghai Institute of Optics and Fine Mechanics, State Key Laboratory of High Field Laser Physics, Shanghai 201800, China; IFSA Collaborative Innovation Center, Shanghai Jiao Tong University, Shanghai 200240, China;
e-mail: lengyuxin@mail.siom.ac.cn, ruxinli@mail.shcnc.siom.ac.cn

Received 14 February 2017
Kvantovaya Elektronika **47** (3) 179–183 (2017)
Submitted in English

GVD, TOD and FOD by inserting a grism pair into a standard chirped-pulse amplification system between a stretcher and a compressor in a 200-TW laser system [16]. The pulse duration was reduced to 28 fs, and the spectral phase distortion over the spectrum was reduced to 4 rad. Because of the alignment and fabrication errors of the dispersion components, the pulse duration measured was 1.3 times longer than the theoretical value, and the spectral distortion was 3 rad larger than that theoretically predicted.

In this work, to achieve the dispersion management of the front end in the Shanghai superintense ultrafast laser facility (SULF), which is a Ti:sapphire based CPA facility, we use a grism pair to reduce high-order dispersion introduced by optical materials. The alignment of the grism pair is implemented by controlling the far-field pattern of the output beam of the grism. The far-field pattern provides two-dimensional information about the uncompensated angular dispersion. An experiment is carried out to verify the effects of dispersion compensation in the front end.

2. Background and simulations

A double CPA architecture is employed in the laser facility. The first CPA is a commercial 1-kHz CPA laser system (Astrella, Coherent Inc.) delivering 95-μJ-level, sub-30-fs pulses. The pulses are injected into the pulse cleaner based on cross-polarised wave (XPW) generation [17, 18]. The spectral width of the cleaned pulses is over 65 nm (FWHM), which can support sub-15-fs-pulse duration. The cleaned pulses with an energy of 20 μJ are stretched to about 2 ns by an Öffner-triplet-type stretcher with a 1480 lines mm^{-1} gold-coated grating (Jobin Yvon, Inc.). The stretcher has an eight-pass configuration. The radii of curvature of the concave and convex mirrors are 1600 mm and 800 mm, respectively. The incident angle is 50°, and the grating is 300 mm away from the centre of the sphere. In fact, the stretcher is not aberration-free when the grating is off the centre of the imaging system. The stretcher has few aberrations with larger radii of curvature of the concave.

After passing through the stretcher, the stretched pulse is amplified in the regenerative amplifier. A spectral shaper is inserted into the regenerative amplifier, in order to prevent spectrum gain narrowing and pre-compensate for spectrum red-shift in the following amplifiers. After the regenerative amplifier, the laser beam passes through two Pockels cells (5046D, FastPulse Inc.), and the repetition rate changes to 1 Hz. The laser pulse is amplified to 7 J after three-stage amplification. To verify that the laser pulse can be compressed for, a pre-compressor is placed after the third amplifier. The compressor has a double-pass configuration consisting of two 1480 lines mm^{-1} gold-coated gratings (Jobin Yvon, Inc.). The size of the first grating is 165 × 220 mm, and the second grating is 190 × 350 mm. Because of the material dispersion caused by the optical materials during the amplification stage, the grating compressor and the stretcher could not match well to obtain a flat spectral phase over the spectral bandwidth. Table 1 shows the length of the optical materials used in the laser system. The Ti:sapphire and KD^*P crystals contribute most to the dispersion. We use the Sellmeier equation to calculate the dispersion introduced by the optical materials [19, 20]. The second, third and fourth order dispersions are 1.2217×10^5 fs^2, 9.7637×10^4 fs^3 and -4.2483×10^4 fs^4, respectively.

Table 1. Lengths of optical materials in the laser system.

Material	Length/mm	Material	Length/mm
K 9	20	FS	543.4
TGG	40	e-sapphire	1016
e-calcite	80	KD^*P	960

Note: TGG is terbium gallium garnet; e-calcite and e-sapphire indicate dispersion along the extraordinary axis of the crystal; FS is fused silica; and KD^*P is deuterated potassium dihydrogen phosphate.

To balance the spectral phase in the laser system, a double-pass grism pair is inserted into the petawatt laser system to compensate for the residual dispersion up to the fourth order. The grisms are inserted between the stretcher and regenerative amplifier. In general, the distance between the grating and the prism is extremely small, and has a negligible effect on the spectral phase. The configuration of the grism is shown in Fig. 1. The anti-symmetrically positioned grism pair is used to provide negative dispersion. The parameter L_{in}, which is referred to as the insertion amount [21], is the distance from the apex point to the position where the laser beam enters the first grism, and L_x is the insertion amount of the centre wavelength on the second grism. The retroreflector sends the beam back along the same path but at a different height. The homemade grism pair consists of two 50 × 50 mm reflection gratings (Richardson gratings), two antireflection-coated SF11 prisms with hypotenuses of 50 mm and 80 mm, respectively, and a homemade antireflection-coated N-BK7 right-angle prism with a hypotenuse of 50 mm. The following parameters are used in our design: the apex angle of the prism, $\alpha = 20°$; the insertion amount, $L_{in} = 20$ mm; the insertion amount of the second grism, $L_x = 40$ mm; grating groove density, 300 lines mm^{-1}; and grism separation, $L_{gap} = 40$ mm. The function of the grism pair is to correct the high order dispersion, especially the fourth order. The dispersion of the grisms can be tuned by adjusting the incident angle and the separation between the grisms.

Given a certain incident angle of the beam, the spectral phase of the grism pair can be calculated using the ray tracing method [22]. Then, we can adjust the incident angle and the grating separation in the compressor to cancel the second-

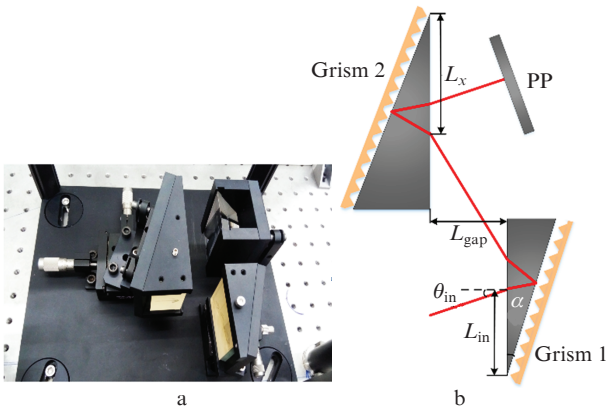

Figure 1. (a) Photograph of the grisms in the laser system and (b) layout of the grisms:
(RM) retro-reflecting roof mirror (retroreflector); (θ_{in}) angle of incidence of the beam; (L_{in}) insertion amount; (L_{gap}) vertical distance between two grisms; (L_x) insertion amount of the centre wavelength.

and third-order dispersion of the laser system. The optimal angle of diffraction and the slant distance between the gratings at the centre wavelength can be expressed as [23]

$$\beta_c = \sin^{-1}\left[\frac{\sqrt{4B^2 + (\lambda_0/d)^2} - \lambda_0/d}{2B}\right], \quad (1)$$

$$L_c = \frac{2\pi c^2 d^2 \cos^2\beta_c}{\lambda_0^3}(\varphi_2^S + \varphi_2^G + \varphi_2^M). \quad (2)$$

Here,

$$B = -1 - \frac{2\pi c}{3\lambda_0}\frac{\varphi_3^S + \varphi_3^G + \varphi_3^M}{\varphi_2^S + \varphi_2^G + \varphi_2^M}; \quad (3)$$

d is the grating groove period; λ_0 is the centre wavelength; c is the velocity of light in a vacuum; φ_2 and φ_3 are the second- and third-order dispersion terms; and the superscripts S, G and M denote the stretcher, grisms and optical materials in the amplifier.

We can then calculate the residual fourth-order dispersion (RFOD) of the system, and estimate whether the value equals zero. Figure 2 shows the RFOD as a function of the incident angle of the grisms. For an incident angle of $\theta_{in} = -0.44°$, the RFOD amount equals zero, which means that GVD, TOD and FOD will be completely compensated for in the front end. One can see from Fig. 2 that the RFOD is very sensitive to the incident angle. In this case, the incident angle and the grating separation of the compressor are 50.63° and 2436 mm, respectively. In general, the alignment of the grism pair is extremely important: slight non-parallelism of the grism pair will introduce an angular chirp and cause an enlargement of the focal spot.

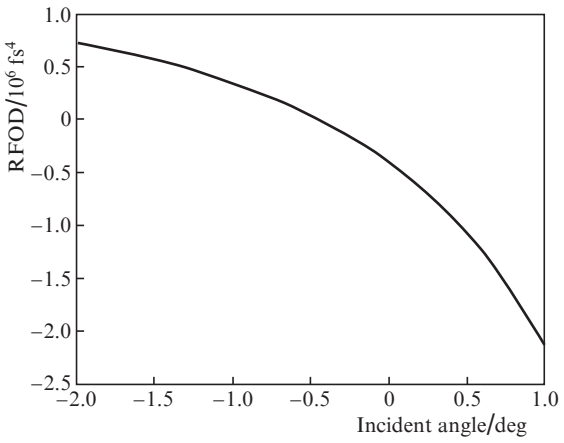

Figure 2. Residual fourth-order dispersion as a function of the incident angle of the grisms.

3. Alignment of the grisms

In order to accurately align the grism pair, a method of far-field monitoring is applied [24]. The experimental configuration is shown in Fig. 3. The incoming beam with an energy of 5.4 μJ and a diameter of 6 mm from the stretcher is injected into the grism pair by M1, and passes through Grism 1 and Grism 2. A mask with holes is inserted between Grism 2 and the retroreflector to obtain two narrowband spectral components. The retroreflector reflects the laser beam back at a different height. The two components are then recombined, and reflected by M2. The output beam is focused by a lens with a 1500 mm focal length. A CCD camera (BeamGage, Ophir Photonics) is placed in the focus plane of the lens. When there are no alignment errors, the focal spots of the two spectral components are coincident with each other. However, when Grism 2 has deviations around the x axis or z axis with respect to Grism 1, the foci of the two components will be separated in the y direction. When Grism 2 is rotated around the y axis with respect to Grism 1, the foci of the two components will be separated in the x direction.

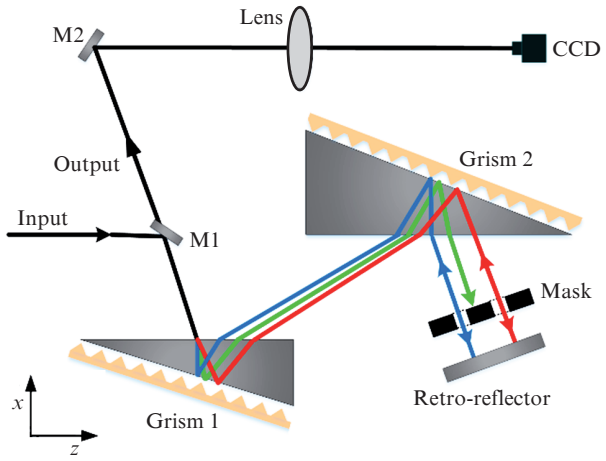

Figure 3. Optical setup for the alignment of the grism pair (top view); M1 and M2 are mirrors. The incoming and output beams do not overlap in the y direction.

The parallelism of the grism pair can be achieved in a stepwise manner. The grism pair is installed in the geometrical position and Grism 2 is rotated around the z axis so that the diffracted beam and the incoming beam are in the same horizontal plane. The focus of the output beam is illustrated in Fig. 4a. It is evident that the focus spot is elongated. The separation of the two foci is about 500 μm. Then, the parallelism of the grism pair is aligned by rotating Grism 2 around the y axis until the foci of the two spectral components merge into one spot as illustrated in Fig. 4b, with Grism 1 being fixed. The alignment of the grism pair can be thus accomplished. The diameter of the focal spot is 255 μm, which is only 1.05 times the diameter of the Airy disk. In fact, the seed pulse has

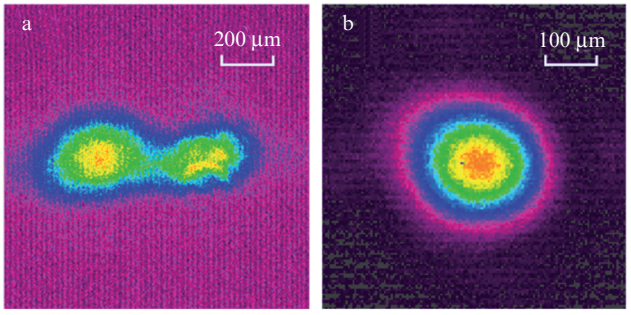

Figure 4. Patterns of the output beam inn the focal plane (a) in the presence of alignment errors and (b) after their correction.

passed through the Öffner stretcher before being injected into the grism pair, and the Öffner stretcher has some nonnegligible chromatic aberration, and hence, the focal spot is not ideal.

4. Results and discussions

The pre-compressor of the front end is operated in the air. To avoid nonlinear effects caused by the laser pulse propagating in the air, the laser beam is reflected by the fused silica plate twice before being injected into the compressor. Then, the compressor is optimised again to obtain the shortest pulse duration. The method proposed in [25] would be beneficial for the alignment procedure. The compressor throughput efficiency is measured to be over 68%. We use a commercial Wizzler system (Fastlite, France) to measure the pulse duration and the spectral phase. A small fraction of the compressed pulses are sent to Wizzler, and the measurement results are shown in Fig. 5. Owing to the spectral shaper used in the regenerative amplifier, the bandwidth of the compressed pulse is more than 100 nm [curve (*1*) in Fig. 5a]. The measured phase [curve (*2*) in Fig. 5a] is the pulse phase distortion introduced by the residual uncompensated high-order dispersion, which is less than 2.25 rad. Curve (*3*) is the result of the fitted phase computed by the Wizzler software. The temporal profile of the compressed pulse is shown in Fig. 5b. The typical duration of the compressed pulse is 22.4 fs (FWHM), while the calculated duration of the FTL pulse [curve (*2*)] is 21.5 fs (FWHM). The retrieved pulse exhibits wings at a level of lower than 10%.

The long-term stability of the pulse duration is measured after the alignment. We measure the variation in the pulse duration for 100 shots and the result is shown in Fig. 6. The pulse duration jitters over time. The mean duration is 22.38 fs, and the corresponding standard deviation is only 0.13 fs. The main factors affecting the pulse duration are the environment and the beam pointing stability. The residual uncompensated high-order dispersion may be caused by the calculation errors of the dispersion. In fact, the dispersion of dielectric mirrors is uncertain. Further, we calculate the material dispersion using the Sellmeier equation. However, the Sellmeier equation is an empirical equation, and thus the calculated dispersion is different from the true value. These factors will affect the calculation accuracy.

For a comparison, another experiment is performed with the grism pair removed, and the compressor is optimised again to obtain the shortest pulse duration. The inset in Fig. 5b illustrates the temporal profile of the compressed pulse. The typical pulse duration is 26.5 fs (FWHM), and the retrieved pulse exhibits wings at a level of higher than 20%. Experimental results show that it is very important to insert a grism pair in the front end to obtain a near FTL pulse.

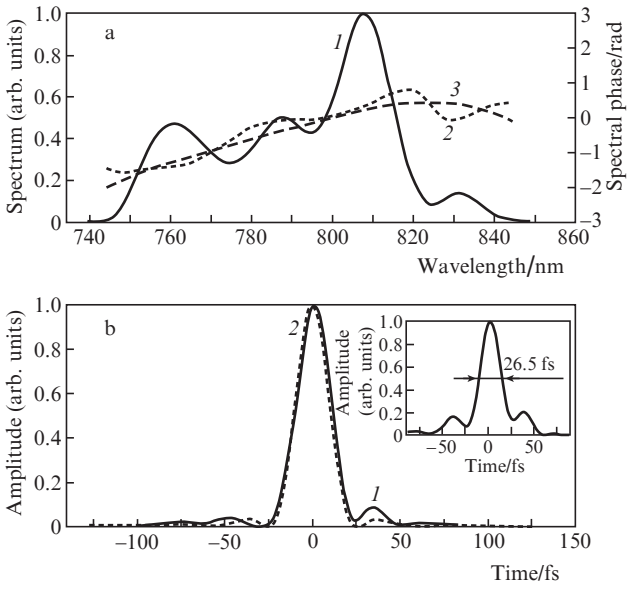

Figure 5. Characteristics of the compressed beam: (a) input spectrum (*1*), measured phase of the pulse (*2*) and fitted phase (*3*) as well as (b) temporal profile of the measured pulse (*1*) and transform-limited pulse (*2*). The inset illustrates the temporal profile of the optimal compressed pulse without grisms.

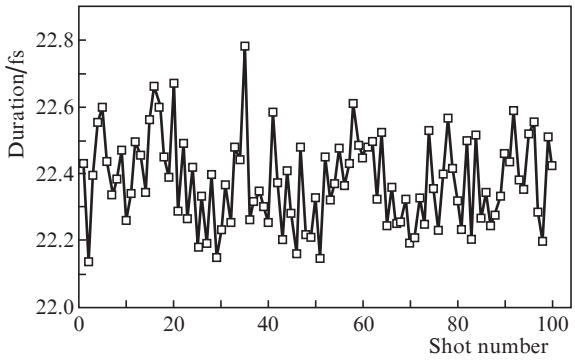

Figure 6. Variation in pulse durations for 100 shots.

5. Conclusions

A grism pair is used to reduce the high-order dispersion introduced by the optical materials of the CPA Ti:sapphire system. The alignment of the grism can be implemented by controlling the far-field pattern of the output beam of the grism, which provides two-dimensional information about the uncompensated angular dispersion. A pre-compressor is fabricated after the amplifier, which delivers laser pulses with an energy of 7 J at a 1-Hz repetition rate. Experimental results demonstrate that the compressed pulse duration is reduced to 22.4 fs, which is only 1.04 times that of the FTL pulse, and the residual phase over the spectral bandwidth is less than 2.25 rad. The grism pair and its alignment method will greatly benefit the dispersion compensation of the SULF in the future.

Acknowledgements. This work was supported by the National Basic Research Programme of China (Grant No. 011CB808101), the Strategic Priority Research Programme of the Chinese Academy of Sciences (Grant No. XDB16), and National Natural Science Foundation of China (Grant Nos 61521093, 61078037, 11127901, 11134010, 61205208 and 11204328).

References

1. Strickland D., Mourou G. *Opt. Commun.*, **55**, 447 (1985).
2. Dubietis A., Jonušauskas G., Piskarskas A. *Opt. Commun.*, **88**, 437 (1992).

3. Lozhkarev V.V., Freidman G.I., Ginzburg V.N., Katin E.V., Khazanov E.A., Kirsanov A.V., Luchinin G.A., Mal'shakov A.N., Martyanov M.A., Palashov O.V., Poteomkin A.K., Sergeev A.M., Shaykin A.A., Yakovlev I.V. *Laser Phys. Lett*., **4**, 421 (2007).
4. Phuoc K.T., Cord S., Thaury C., et al. *Nat. Photon*., **6**, 308 (2012).
5. Perry M.D., Pennington D., Stuart B.C., et al. *Opt. Lett*., **24**, 160 (1999).
6. Aoyama M., Yamakawa K., Akahane Y., Ma J., Inoue N., Ueda H., Kiriyama H. *Opt. Lett*., **28**, 1594 (2003).
7. Danson C., Hillier D., Hopps N., Neely D. *High Power Laser Sci. Eng.*, **3** (1), e3 (2015).
8. Papadopoulos D.N., Zou J.P., Blanc C.L., Chériaux G., Georges P., Druon F., Mennerat G., Ramirez P., Martin L., Fréneaux A., Beluze A., Lebas N., Monot P., Mathieu F., Audebert P. *High Power Laser Sci. Eng.*, **4**, e34 (2016).
9. Chu Y., Liang X., Yu L., Xu Y., Xu L., Ma L., Lu X., Liu Y., Leng Y., Li R., Xu Z. *Opt. Express*, **21**, 29231 (2013).
10. Yakovlev I.V. *Quantum Electron*., **44**, 393 (2014) [*Kvantovaya Elektron*., **44**, 393 (2014)].
11. Sun Z., Chai L., Zhang Z., Wang C., Zhang W., Xie X., Huang X., Yuan X. *Opt. Laser Technol*., **39**, 29 (2007).
12. Verluise F., Laude V., Cheng Z., Spielmann C., Tournois P. *Opt. Lett*., **25**, 575 (2000).
13. Zeek E., Maginnis K., Backus S., Russek U., Murnane M., Mourou G., Kapteyn H., Vdovin G. *Opt. Lett*., **24**, 493 (1999).
14. Gibson E.A., Gaudiosi D.M., Kapteyn H.C., Jimenez R., Kane S., Huff R., Durfee C., Squier J. *Opt. Lett*., **31**, 3363 (2006).
15. Forget N., Grabielle S., Tournois P. *Proc. CLEO 2014* (San Jose, Cal.: OSA, 2014) SW1E.6.
16. Li Z., Wang C., Li S., Xu Y., Chen L., Dai Y., Leng Y. *Opt. Commun*., **357**, 71 (2015).
17. Xu Y., Leng Y., Guo X., Zou X., Li Y., Lu X., Wang C., Liu Y., Liang X., Li R., Xu Z. *Opt. Commun*., **313**, 175 (2014).
18. Jullien A., Albert O., Chériaux G., Etchepare J., Kourtev S., Minkovski N., Saltiel S.M. *Opt. Express*, **14**, 2760 (2006).
19. Ghosh G. *Appl. Opt*., **36**, 1540 (1997).
20. http://www.unitedcrystals.com/KDPProp.html.
21. Zheng J., Zacharias H. *Appl. Phys. B*, **96**, 445 (2009).
22. Dou T.H., Tautz R., Gu X., Marcus G., Feurer T., Krausz F., Veisz L. *Opt. Express*, **18**, 27900 (2010).
23. Kane S., Squier J. *J. Opt. Soc. Am. B*, **14**, 1237 (1997).
24. Liu F., Liu X., Wang Z., Ma J., Liu X., Zhang L., Wang J., Wang S., Lin X., Li Y., Chen L., Wei Z., Zhang J. *Appl. Phys. B*, **101**, 587 (2010).
25. Li S., Li Z., Wang C., Xu Y., Li Y., Leng Y., Li R. *Opt. Eng*., **55**, 086105 (2016).